Physiological and metabolomic changes during *ex-vivo* lung perfusion according to temperature of the perfusate.

Jee Won Suh

Department of Medicine

The Graduate School, Yonsei University

Physiological and metabolomic changes during *ex-vivo* lung perfusion according to temperature of the perfusate.

Directed by Professor Hyo Chae Paik

The Doctoral Dissertation
submitted to the Department of Medicine,
the Graduate School of Yonsei University
in partial fulfillment of the requirements for the degree
of Doctor of Philosophy

Jee Won Suh

June 2022

This certifies that the Doctoral Dissertation of Jee Won Suh is approved

---

Thesis Supervisor: Hyo Chae Paik

Thesis Committee Member#1: Moo Suk Park

Thesis Committee Member#2: Jae Woo Kim

Thesis Committee Member#3: Hyo Sup Shim

Thesis Committee Member#4: Seokjin Haam

The Graduate School
Yonsei University

June 2022

ACKNOWLEDGEMENTS

I would like to thank all my senior professors, colleagues, juniors, and family members, who supported and guided me from becoming a doctor to a thoracic surgeon.

I would like to thank Professor Hyo Chae Paik for guiding me as a thoracic surgeon, and teaching me to move forward even in difficult situations. Moreover, I am thankful to Professor Seokjin Haam, Professor Moo Suk Park, Professor Jae Woo Kim, and Professor Hyo sup Shim for their guidance in this study.

Most importantly, I would like to express my gratitude and love to my family and friends, who have supported and loved me till date.

TABLE OF CONTENTS

ABSTRACT ····· 1

I. INTRODUCTION ····· 3
II. MATERIALS AND METHODS ····· 6
1. Animals ····· 6
2. Experimental animal protocol for EVLP ····· 6
3. Evaluation of pulmonary function during EVLP ····· 8
4. Histopathological evaluation of lung tissue ····· 8
5. Metabolic profiling by CE-TOFMS ····· 8
A. Sample preparation ····· 8
B. CE-TOFMS conditions ····· 9
C. Data processing ····· 9
6. RNA extraction and qPCR ····· 10
7. Statistical analysis ····· 12
III. RESULTS ····· 13
1. Lung function during EVLP ····· 13
2. Histological analysis ····· 14
3. Cytokine and protein expression ····· 15
4. Metabolite analysis ····· 16
A. Glucose metabolism ····· 19
B. TCA cycle ····· 22
5. mTORC- HIF1α- NLRP3 inflammasome pathway signaling ····· 24
IV. DISCUSSION ····· 26
V. CONCLUSION ····· 31

REFERENCES ····· 32

APPENDICES ····· 38
ABSTRACT (IN KOREAN) ····· 39

LIST OF FIGURES

Figure 1. Protocol for EVLP. ····· 7
Figure 2. Analyses of EVLP parameters and lung graft pathologic findings. ····· 13
Figure 3. LIS score and histological findings upon H&E staining. ····· 14
Figure 4. Proinflammatory cytokine and caspase 3 mRNA expression levels in samples from sham, control, and study groups. ····· 16
Figure 5. Principal component analysis. ····· 17
Figure 6. Metabolite levels in glycolysis pathways. ····· 21
Figure 7. Metabolite levels in TCA cycle. ····· 23
Figure 8. Expression level of mTORC, HIF-1α, and NLRP3 in samples from sham, control, and study groups. ····· 24

LIST OF TABLES

Table 1. Primer sequences for qPCR ····· 11
Table 2. Metabolites showing 10 highest and lowest loading factors in PCA ····· 17

ABSTRACT

Physiological and metabolomic changes during *ex-vivo* lung perfusion according to temperature of the perfusate

Jee Won Suh

Department of Medicine
The Graduate School, Yonsei University

(Directed by Professor Hyo Chae Paik)

Purpose: *Ex-vivo* lung perfusion (EVLP) is a useful technique for evaluating and repairing donor lungs for transplantation; it can increase lung utility rates and reduce graft dysfunction due to ischemic reperfusion injuries. However, studies demonstrating the effect of perfusate temperatures on graft function are limited. This study aimed to examine the effects of subnormothermic perfusate temperature during EVLP on the donor lung ischemic reperfusion injury in the viewpoint of lung function and histology using metabolomics.

Material and Methods: Fifteen male Sprague–Dawley rats were randomly divided into three groups, namely no treatment (sham group, n = 5), normothermic EVLP (37 °C, control group, n = 5), and subnormothermic EVLP (30 °C, study group, n = 5). Lung function analyses, in terms of oxygen capacity (OC), compliance, and pulmonary vascular resistance (PVR), were performed. The expression levels of inflammatory cytokines were evaluated. Metabolome analysis was performed on lung tissues from each group using capillary electrophoresis time-of-flight mass spectrometry.

Results: Functional parameters, including OC and PVR, were significantly

superior in the study group than in the control group during EVLP. Expression levels of inflammatory cytokines, such as IL-6, 18, 1ß, and TNF-α, were significantly lower in the study group than in the control group. Metabolome analysis showed glycolysis to be significantly decreased in the study group than in the control group.

Conclusion: Compared to normothermic EVLP, subnormothermic EVLP improves the lung graft function by decreased expression of proinflammatory cytokines and suppressed glycolytic activities. This could be explained by inhibition the mTORC1-HIF1α pathway in subnormothermic EVLP.

Key words: *ex-vivo* lung perfusion, temperature, lung transplantation, metabolomics, glycolysis

Physiological and metabolomic changes during *ex-vivo* lung perfusion according to temperature of the perfusate.

Jee Won Suh

Department of Medicine
The Graduate School, Yonsei University

(Directed by Professor Hyo Chae Paik)

I. INTRODUCTION

Lung transplant is the only curative treatment for patients with end-stage lung disease. Owing to the shortage of organ donors, due to the low procurement rate of lungs from brain death donors, only 15–25% of potential donor lungs are actually transplanted [1]. The low procurement rate of brain-dead donor lungs is attributed to aspiration-associated injuries, barotraumas, and ventilator-associated pneumonia during the brain death process [2]. Considering the increased waiting-list mortalities due to low procurement rate, alternative options of marginal and circulatory death donors have emerged. *Ex-vivo* lung perfusion (EVLP) is a method to increase lung utility rates and reduce graft dysfunction due to ischemic reperfusion injuries.

EVLP is a well-known platform for the evaluation and preservation of donor function, where donors do not meet standard donor criteria. Currently, protocols from clinically available EVLP systems – the Lund, Toronto, and Organ Care System – are mainly used with normothermic (37 °C) EVLP [3]. In this method, the lung is perfused and ventilated *ex vivo* at body temperature to mimic physiological conditions [4]. From the time the concept of EVLP emerged until

recently, EVLP has performed under normothermic or near normothermic conditions, since hypothermia could reduce metabolic functions, and preclude meaningful evaluation and recovery [5]. Although normothermic EVLP leads to increased waste and proinflammatory cytokine production [6-8], it has been shown to be safe and reliable for the repair of damaged organs [9-11], and for improved function of marginal donor lungs and post-transplant outcomes [4,12-15].

There are limited studies for the effect of perfusate temperature in EVLP on donor lung function. Several studies have evaluated subnormothermic or hypothermic machine perfusion in kidney and liver transplants. Based on better nutrient supplies and endothelial protection [16], hypothermic machine perfusion (HMP) is considered the gold standard for circulatory death kidney transplantation [17]. Furthermore, HMP stimulates aerobic metabolism while limiting organ metabolism and oxygen demand at low temperatures in liver transplantation [16]. Recent studies have observed the effect of perfusate temperature on EVLP in lung transplants. Subnormothermic EVLP showed significantly lower energy consumption and inflammatory response compared to normothermic EVLP, and protective effect on the lung was maintained in a rat model of donation after circulatory death [6-8,18].

Metabolomic analysis, measuring a large number of metabolites, quantitatively assesses the dynamic responses to physiological and pathological changes [19]. Metabolites may provide important information about the extent of tissue repair or damage [20]. Oxidative stress and specific energy metabolites emerge as a result of low perfusate temperatures [20-22]. These metabolites have been used to monitor organ function and perfusion injury in organ transplants [20].

Based on previous studies, the purpose of this study is to investigated the mechamism by which subnormothermia during EVLP is associated with a protective effect against IR injuries in the rat EVLP model. Further, the study aimed to investigate the changes occurring in lung graft, after subnormothermic EVLP and normothermic EVLP, focusing on energy metabolism and

inflammatory pathways.

II. MATERIALS AND METHODS

1. Animals

Male Sprague Dawley rats (DBL, Eumseong, Korea) weighing 280–320 g were used in this study. All experimental and animal care procedures were conducted in accordance with the Laboratory Animal Welfare Act, and the Guide for the Care and Use of Laboratory Animals provided by the Ajou University Institutional Animal Care and Use Committee (IACUC No. 2016-0047), and were in compliance with the 'Guide for the Care and Use of Laboratory Animals' by the National Institutes of Health (NIH Publication No. 86-23, revised 1996).

2. Experimental animal protocol for EVLP

Fifteen rats were randomly assigned to one of the three following groups: no treatment (sham group, n = 5), normothermic (37 °C) EVLP (control group, n = 5), and subnormothermic (30 °C) EVLP (study group, n = 5). The basic anesthesia and EVLP protocol were as follows: rats were subjected to isoflurane inhalation (Hana Pharm, Seoul, Korea), followed by tracheotomy, and received mechanical ventilation with O_2 and 3% isoflurane. A 20 ml preservation solution (Perfadex Plus; XVIVO, Göteborg, Sweden) containing 3 μg of prostaglandin E1 (Alpostin; Dongkook Pharmaceutical, Seoul, South Korea) was infused through the pulmonary artery (PA), after which the lungs were harvested. The lung grafts were procured and preserved at 4 °C for 1 h. After cannulation and during cold ischemia, EVLP was applied for 4 h according to a previously published protocol [23]. Briefly, EVLP was performed using a commercially available rodent system (IL-2 isolated perfused rat or guinea pig lung system; Harvard Apparatus, Holliston, MA, USA) [24]; EVLP for basic experiments was performed in the same manner as described previously [24]. During EVLP, the lungs were ventilated with air, perfused with STEEN solution (XVIVO Perfusion AB, Gothenburg, Sweden), deoxygenated with 6% O_2, 8% CO_2, and balanced N_2, and supplemented with 50

mg methylprednisolone (Solu-Medrol; Pfizer, Inc., New York, NY, USA) and 50 mg cephalosporin (Cefazolin; West-Ward Pharmaceuticals Corp., Eatontown, NJ, USA). Ventilation was set in a pressure-controlled mode (15 cm H_2O) with 5 cm H_2O positive end-expiratory pressure and a respiratory rate of 30 breaths/min. Perfusion flow was initiated when 10% of the target flow was reached, and was then gradually increased for 1 h to a target flow rate that was calculated as 20% of the cardiac output (75 mL/min/250 g rat body weight). In the control group, the perfusate temperature was gradually increased to 37 °C for 20 min and maintained at 37 °C throughout the EVLP period. In the study group, the perfusate temperature was increased to 30 °C for 10 min and maintained at 30 °C throughout the EVLP period (Figure 1).

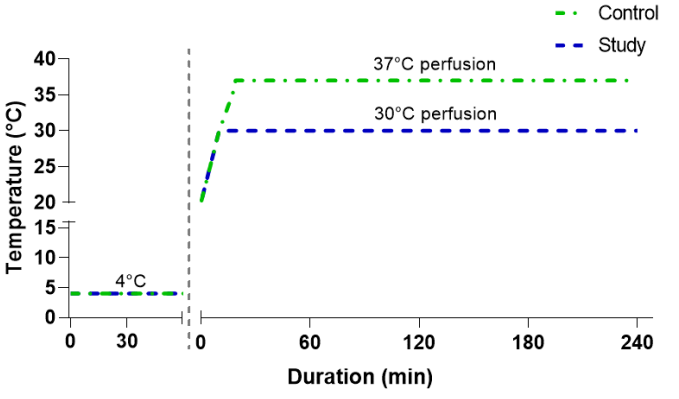

4℃ Cold static preservation	*Ex-vivo* lung perfusion	Sacrificed
	Hourly measurement of functional parameter	Histological evaluation Metabolic profiling qPCR

Figure 1. Protocol for *ex vivo* lung perfusion (EVLP). The lung grafts were preserved at 4 °C for 1 h. Thereafter, sham group was preserved at 4 °C, whereas EVLP was applied to control and study groups for 4 h at 37 °C or 30 °C, respectively.

3. Evaluation of pulmonary function during EVLP

Lung function parameters were measured hourly during EVLP. Mechanical ventilation was performed with fraction of inspired oxygen (FiO_2) = 1.0 for 10 min before each measurement. The functional parameters measured included oxygen capacity (OC; [left atrial (LA) perfusate partial pressure of oxygen (PO_2)-pulmonary arterial (PA) perfusate PO_2]/FiO_2), which was calculated using arterial blood gas analysis, pulmonary vascular resistance (PVR; [PA pressure-LA pressure] × 80/pulmonary arterial flow), dynamic lung compliance (Cdyn), and peak airway pressure (PAP).

4. Histopathological evaluation of lung tissue

After 4 h of EVLP, the upper right lobes of the lungs were fixed with 10% buffered formalin and prepared for histopathological evaluation using hematoxylin and eosin staining. Histopathological analysis was performed by a blinded pathologist using the lung injury severity (LIS) score system [25,26]. Lung injuries are measured using a 5-point (0 to 4 point) scale according to the assessment of i) alveolar congestion; ii) hemorrhage; iii) infiltration of aggregation of neutrophils in the airspace or vessel wall; and iv) thickness of alveolar wall/hyaline membrane formation, separately. Finally, the LIS score is calculated by summation of the scores.

5. Metabolic profiling by capillary electrophoresis time-of-flight mass spectrometry (CE-TOFMS)

A. Sample preparation

The samples for each group (sham, control, and study) were placed in a homogenization tube with zirconium beads (5 mm φ and 3 mm φ); 750 μL of 50% acetonitrile in Milli-Q water (v/v) containing internal standards (20 μM) were added to the tube. The sample was completely homogenized at 1,500 rpm at 4 °C,

4 times for 2 min each, using a bead shaker. Following this, 750 μL of 50% acetonitrile in Milli-Q water (v/v) were added to the mixture and homogenized once again. The homogenate was centrifuged at 2,300 × *g*, at 4 °C for 5 min, and the upper aqueous layer was centrifugally filtered at 4 °C through a 5-kDa cut-off filter (ULTRAFREE-MC-PLHCC, Human Metabolome Technologies, Yamagata, Japan) to remove macromolecules. The filtrate was evaporated to dryness, under vacuum, and reconstituted in Milli-Q water for CE-TOFMS analysis.

B. CE-TOFMS conditions

CE-TOFMS was performed using an Agilent CE Capillary Electrophoresis System (Agilent Technologies Inc., Waldbronn, Germany). Cationic metabolites were analyzed using a fused silica capillary column (i.d. 50 μm × 80 cm) with commercial cation electrophoresis buffers (Solution ID: H3301-1001, Human Metabolome Technologies). The sample was injected at a pressure of 50 mbar for 10 s at an applied voltage of 30 kV. Electrospray ionization-mass spectrometry (ESI-MS) was conducted in positive-ion mode with a capillary voltage of 4000 V. The spectrometer scanned the range of mass-to-charge ratio (m/z) of 50–1000.

Anionic metabolites were analyzed using a fused silica capillary column (i.d. 50 μm × 80 cm) with commercial anion electrophoresis buffers (Solution ID: I3302-1023, Human Metabolome Technologies). The sample was injected at a pressure of 50 mbar for 10 s at an applied voltage of 30 kV. ESI-MS was conducted in the negative ion mode with a capillary voltage of 3500 V. The spectrometer scanned the range of m/z ratio of 50–1000.

C. Data processing

Peaks detected in CE-TOFMS analysis were extracted using automatic integration software (MasterHands ver. 2.19.0.2, developed at Keio University), and the extracted data included m/z, migration time (MT), and peak area. Five lung samples from each group (sham, control, and study) were used for the

metabolomic analysis, and 292 peaks (175 in cation and 117 in anion mode) were detected. The peak area was converted to relative peak area, using an equation from a previous study[27]. Putative metabolites were assigned from the Human Metabolome Technologies (HMT) standard library and known-unknown peak library on the basis of m/z (tolerance ±10 ppm[3]) and MT (tolerance ± 0.5 min). If several peaks were assigned to the same candidate, the latter was assigned a branch number. Absolute quantification was performed for the target metabolites. Metabolite concentrations were calculated by normalizing the peak area of each metabolite with respect to the area of the internal standard using standard curves obtained from single-point (100 μM) calibrations. Among the target metabolites, 88 (50 in cation and 38 in anion mode) were detected and quantified. Hierarchical cluster analysis (HCA) and principal component analysis (PCA) were performed using a statistical software (developed at HMT) [27]. The peak profiles with putative metabolites were represented on metabolic pathway maps using VANTED (Visualization and Analysis of Networks containing Experimental Data, http://vanted.ipk-gatersleben.de/) 5 software. The pathway map was prepared based on the metabolic pathways that are known to exist in human cells. Metabolite abundance differences were considered significant when the final corrected value had $P < 0.05$.

6. RNA extraction and qPCR

Quantitative reverse transcription-polymerase chain reaction (qRT-PCR) was performed to evaluate the expression levels of inflammatory cytokines, caspase-3, and enzymes that are associated with glycolysis pathway in each group, along with those of mTORC, HIF-1α, and NLRP3. RNA was extracted from the lung tissues of sham (n = 5), control (n = 5), and study groups (n = 5). Total RNA was isolated from the upper left lobes of the lungs using TRIzol reagent (#TR118, Molecular Research Center Inc., Cincinnati, OH, USA), according to the manufacturer's protocol. For qRT-PCR, total RNA was reverse transcribed using

AMV Reverse Transcriptase (#M0277L, New England Biolabs, Ipswich, MA, USA). The transcript levels of target genes were quantified with 2× KAPA SYBR Fast qPCR Master Mix (#kk4602, Kapa Biosystems, Cape Town, South Africa) using the StepOnePlus™ Real-Time PCR System 510 (Applied Biosystems, Foster City, CA, USA). For each target gene, the transcript level was normalized to that of GAPDH and calculated using the standard ΔΔCT method. The primer sequences are shown in Table 1.

Table 1. Primer sequences for qPCR

Symbol	Forward	Reverse
TNF-α	AAGCTGTCTTCAGGCCAACA	CCCGTAGGGCGATTACAGTC
IL-1ß	GTCTGACCCATGTGAGCTGAA	CAAGGCCACAGGGATTTTGTC
IL-6	TAGTCCTTCCTACCCCAACTTCC	TTGGTCCTTAGCCACTCCTTC
IL-18	TGGAATCAGACCACTTTGGCA	TCTGGGATTCGTTGGCTGTT
Caspase 3	GTGGAACTGACGATGATATGGC	CGCAAAGTGACTGGATGAACC
HK	GACGAACCTGGACTGTGGAAT	TCCTCTCTCCTCTTCACCGC
PFK	ATCCACGACTTGAAGGCCAA	CTGCAGTCGAACACACCTCT

PKM	CCTGATAGCTCGAGAGGCTG	TATAAGAGGCCTCCACGCTG
HIF-1α	ACATCTTCTTCTGCTCCACTAC	CTGGAGATTAGTAATGGCCCAT
mTORC	ACTGTTCCTGTCCATGTA TCTG	GTAGTGGAGCAGAAGAAGATGT
NLRP3	GCCACTATGTACTCAT ACGACA	AGTCAGGGATCTTCACTTTGAG
Caspase 1	AAAGATTCAGTAGGGAACTCCG	TCACAAGACCAGGCATATTCTT
GAPDH	TCTCTGCTCCTCCCTGTTCTA	ATGAAGGGGTCGTTGATGGC

7. Statistical analysis

Functional and histological parameters were expressed as mean ± standard error of the mean. For comparison of lung function parameters, such as OC, PVR, and PAP, repeated measures analysis of variance (ANOVA) was performed. The LIS scores were compared using Fisher's exact test. Statistical analysis of gene expression levels was performed using one-way ANOVA with Tukey's multiple comparison test. All statistical analyses were performed using SPSS software 26 (IBM, USA) and graphic figures were prepared using GraphPad Prism 9 (GraphPad Software, San Diego); statistical significance was set at $p < 0.05$.

III. RESULTS

1. Lung function during EVLP

There were statistically significant differences in functional parameters during EVLP between the control and study groups in terms of OC (1-h control vs. study, 302.2 ± 17.51 vs. 419.4 ± 41.94; 4-h control vs. study, 306.6 ± 35.98 vs. 368.6 ± 68.23, $p < 0.0001$) and PVR (1-h control vs. study, 0.79 ± 0.04 vs. 0.69 ± 0.05; 4-h control vs. study, 1.10 ± 0.11 vs. 0.74 ± 0.06, $p = 0.0002$). There was, however, no significant difference in lung compliance (1-h control vs. study, 0.19 ± 0.03 vs. 0.19 ± 0.01; 4-h control vs. study, 0.18 ± 0.04 vs. 0.18 ± 0.02, $p = 0.7566$) (Figure 2).

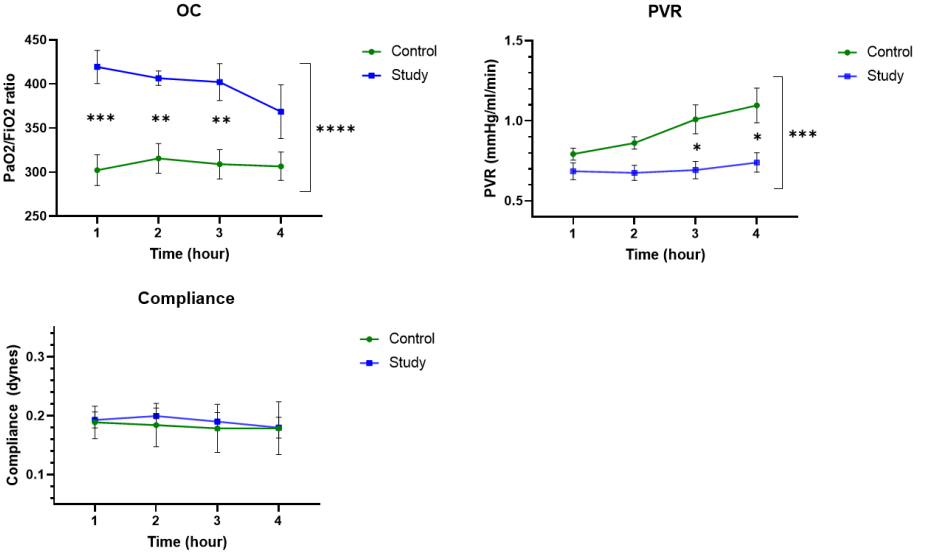

Figure 2. Analyses of *ex-vivo* lung perfusion (EVLP) parameters and lung graft pathologic findings. Functional parameters, including oxygen capacity (OC) ($p < 0.0001$), pulmonary vascular resistance (PVR) ($p = 0.0002$), and dynamic lung compliance (Cdyn) ($p = 0.7566$), were measured every hour during EVLP. Graft function showed statistically significant superiority in terms of OC and PVR in the study than in the control group (* $p < 0.05$, ** $p < 0.01$, *** $p < 0.001$, and ****$p < 0.0001$). OC, oxygen capacity; PVR, pulmonary vascular resistance

2. Histological analysis

There were significant differences in histological changes between the control and study groups, according to the LIS score. The LIS score was 8.75 ± 4.72 in the control group and 1.0 ± 1.16 in the study group (p = 0.0449). Alveolar wall thickening and inflammatory cell accumulation in alveolar space were observed in the control group, while the normal alveolar structure was well maintained in the study group (Figure 3). These results suggested that, the superior graft function of subnormothermic EVLP is due to less inflammatory cell infiltration and alveolar wall thickening. In addition, it could be inferred that the inflammatory response plays a major role of protective effect for perfusate temperature.

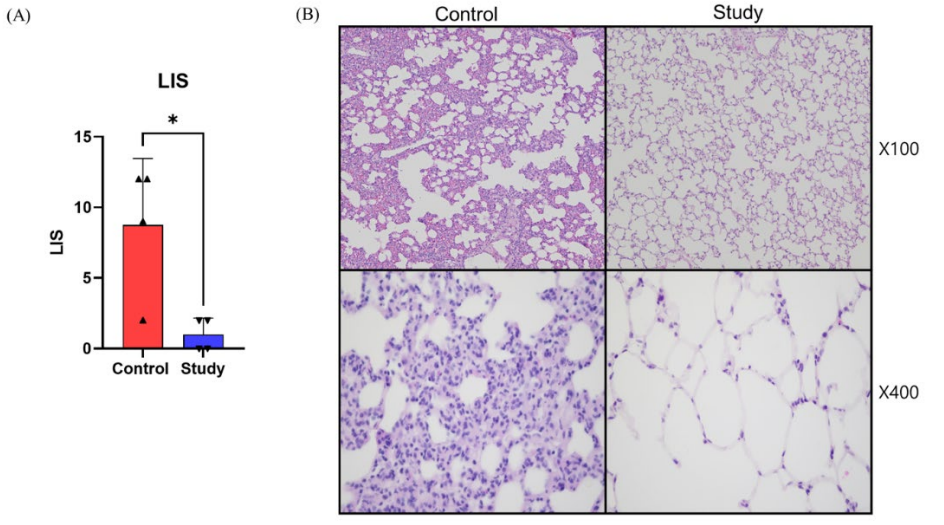

Figure 3. LIS score and histological findings upon H&E staining. (A) LIS score was significantly higher in the control group (p = 0.0449). (B) Histologic findings in graft (H&E, original magnification 100× and 400×); control group (left) and study group (right). Alveolar wall thickening and inflammatory cell accumulation

were observed in the control group. Normal alveolar structure was maintained in the study group.

3. Cytokine and protein expression

The mRNA levels of TNF-α (sham: 1, control: 16.78, study: 2.719; sham vs. control, $p = 0.0005$; sham vs. study, $p = 0.8325$; control vs. study, $p = 0.0013$), IL-1ß (sham: 1, control: 24.18, study: 3.404; sham vs. control, $p = 0.0093$; sham: vs. study, $p = 0.9263$; control vs. study, $p = 0.0183$), IL-6 (sham: 1, control: 19.67, study: 4.978; sham vs. control, $p < 0.0001$; sham: vs. study, $p = 0.2483$; control vs. study, $p = 0.0001$), and IL-18 (sham: 1, control: 12.93, study: 1.807; sham vs. control, $p = 0.0309$; sham: vs. study, $p = 0.9785$; control vs. study, $p = 0.0440$) were significantly higher in the control group than in the sham and study groups. The mRNA levels of caspase-3 (sham: 1, control: 29.87, study: 4.887; sham vs. control, $p = 0.0035$; sham: vs. study, $p = 0.8437$; control vs. study, $p = 0.0095$) were significantly higher in the control group than in the sham and study groups (Figure 4).

These inflammatory cytokine level showed that subnormothermic EVLP has less inflammatory response than normothermic EVLP. It is correlated with histologic finding seen previously, and an experiment was conducted to find the mechanism that related to this inflammatory response.

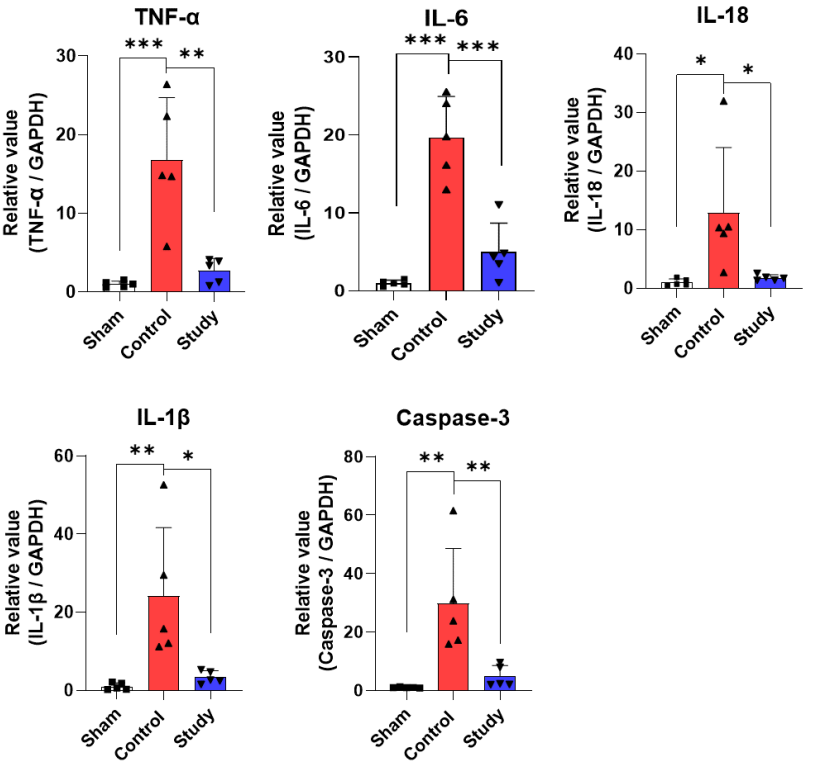

Figure 4. Proinflammatory cytokine and caspase 3 mRNA expression levels in samples from sham, control, and study groups (* $p < 0.05$, ** $p < 0.01$, and *** $p < 0.001$). In the control group, inflammatory cytokines were significantly increased compared to that in sham, and the changes were decreased in the study group to a similar level as in sham.

4. Metabolite analysis

Results of PCA using the detected peaks are shown in Figure 5. The principal component1 (PC1) score was positively correlated to the EVLP effect. Metabolites with large positive factor loadings in PC1 tended to increase in the control and study groups than in the sham group. The PC2 score was positively correlated to the study group. Metabolites that had positive factor loadings in PC2 tended to increase in the study group than in the control group. Details of the

metabolites that 10 highest and lowest loading factors in PCA are described in the Table 2.

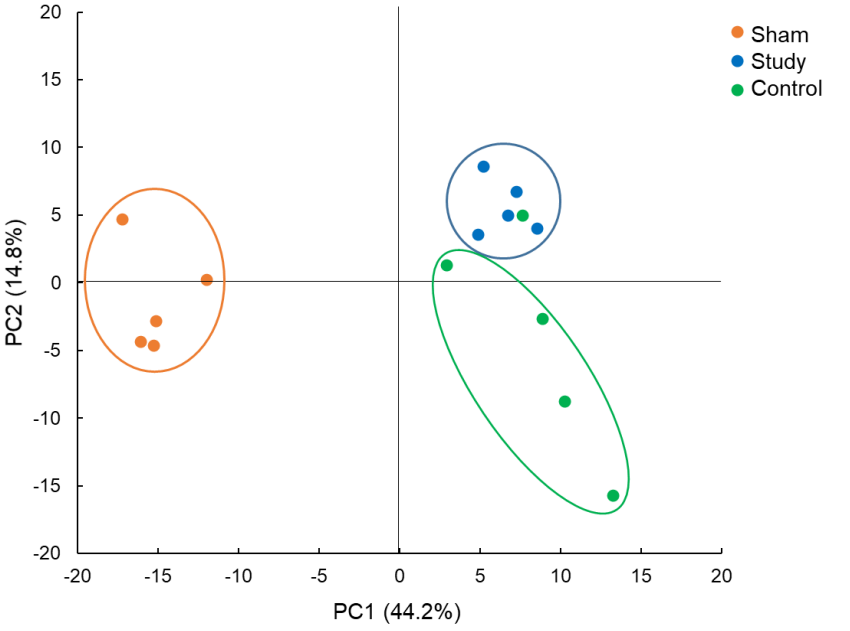

Figure 5. Principal component analysis. Each plot indicates a PCA score for each sample. Percentages shown are the contribution rate for each component.

Table 2. Metabolites showing 10 highest and lowest loading factors in PCA

Component 1 (44.16%)		**Component 2 (14.71%)**	
Metabolite	PCA loading	Metabolite	PCA loading
Octanoic acid	0.98997	Choline	0.92145
N-Acetyltryptophan	0.97772	UDP-N-acetylgalactosamine	0.91567

		UDP-N-acetylglucosamine	
Ibuprofen	0.96209	Glucose 1-phosphate	0.87656
o-Hydroxybenzoic acid	0.95795	XA0065	0.82838
Butyric acid Isobutyric acid	0.95366	γ-Glu-Gly	0.81370
Glycerol	0.91829	Inosine	0.80679
8-Hydroxyoctanoic acid-1 2-Hydroxyoctanoic acid-1	0.89003	Uridine	0.80466
Hexanoic acid	0.88520	Guanosine	0.80181
N^1-Acetylspermidine	0.86887	CMP	0.78705
XC0154	0.86246	*N*-Acetylglucosamine 1-phosphate	0.77429
Leu	-0.99215	4-Methyl-2-oxovaleric acid 3-Methyl-2-oxovaleric acid 2-Oxohexanoic acid	-0.72633
Met	-0.98692	Thiaproline	-0.68469
S-Methylglutathione	-0.98601	2-Oxoisovaleric acid	-0.66474
Ile	-0.98495	Phosphoenolpyruvic acid	-0.63699
Val	-0.97747	Pyruvic acid	-0.63316
Pro	-0.97709	Phosphocreatine	-0.55766
Homoserinelactone	-0.97108	2-Oxoglutaric acid	-0.54713

N, *N*-Dimethylglycine	-0.96416	Isoglutamic acid	-0.51861
S-Adenosylmethionine	-0.96004	Putrescine	-0.50646
S-Lactoylglutathione	-0.95747	1-Methylnicotinamide	-0.48822

With these PCA results, it was possible to infer metabolites and pathways that could classify three groups. PC1 was a metabolite showing a different trend between the sham group and the EVLP group and is related to the TCA cycle and energy conversion (Butyric acid, Isobutyric acid, 8-hydroxyoctanoic acid, 2-hydroxyoctanoic acid, Leucine, Isoleucine, Valine) was the most common. PC2 has shown metabolites that have different trends between the normothermic EVLP group and the subnormothermic EVLP group. Most of these metabolites were carbohydrate metabolism-related metabolites (UDP-N-acetylgalactosamine, UDP-N-acetylglucosamine, Glucose 1-phosphate, *N*-Acetylglucosamine 1-phosphate, Phosphoenolpyruvic acid, Pyruvic acid). As such, it was possible to obtain a clue to select a metabolite that distinguishes characteristics between groups through PCA.

A. Glucose metabolism

The level of metabolites from early step of glycolysis, such as glucose-6-phosphate (G6P, control vs. study, 0.001765 vs. 0.004330; $p = 0.1338$), fructose-6-phosphate (F6P, control vs. study, 0.0003834 vs. 0.0009974; $p = 0.1073$), and fructose-1,6-bisphosphate (F1,6P, control vs. study, 0.001849 vs. 0.002430; $p = 0.6732$) had lower tendency in control group than in study group. Enzymes related to glycolysis, such as hexokinase (HK) and phosphofructokinase (PFK), were significantly expressed in control group than in study group (HK, control vs. study 5.879 vs. 0.2082, $p = 0.0135$; PFK, control vs. study 2.649 vs. 0.3856, $p < 0.0001$) (Figure 6). HK and PFK, key enzymes of glycolysis, were significantly increased in normothermic EVLP, it suggested that glycolytic activity was increased in normothermic EVLP and was alleviated under subnormothermic conditions. Intermediate metabolites of glycolysis were

decreased in normothermic EVLP, it reflects high glycolytic activity and depletion of intermediate metabolites.

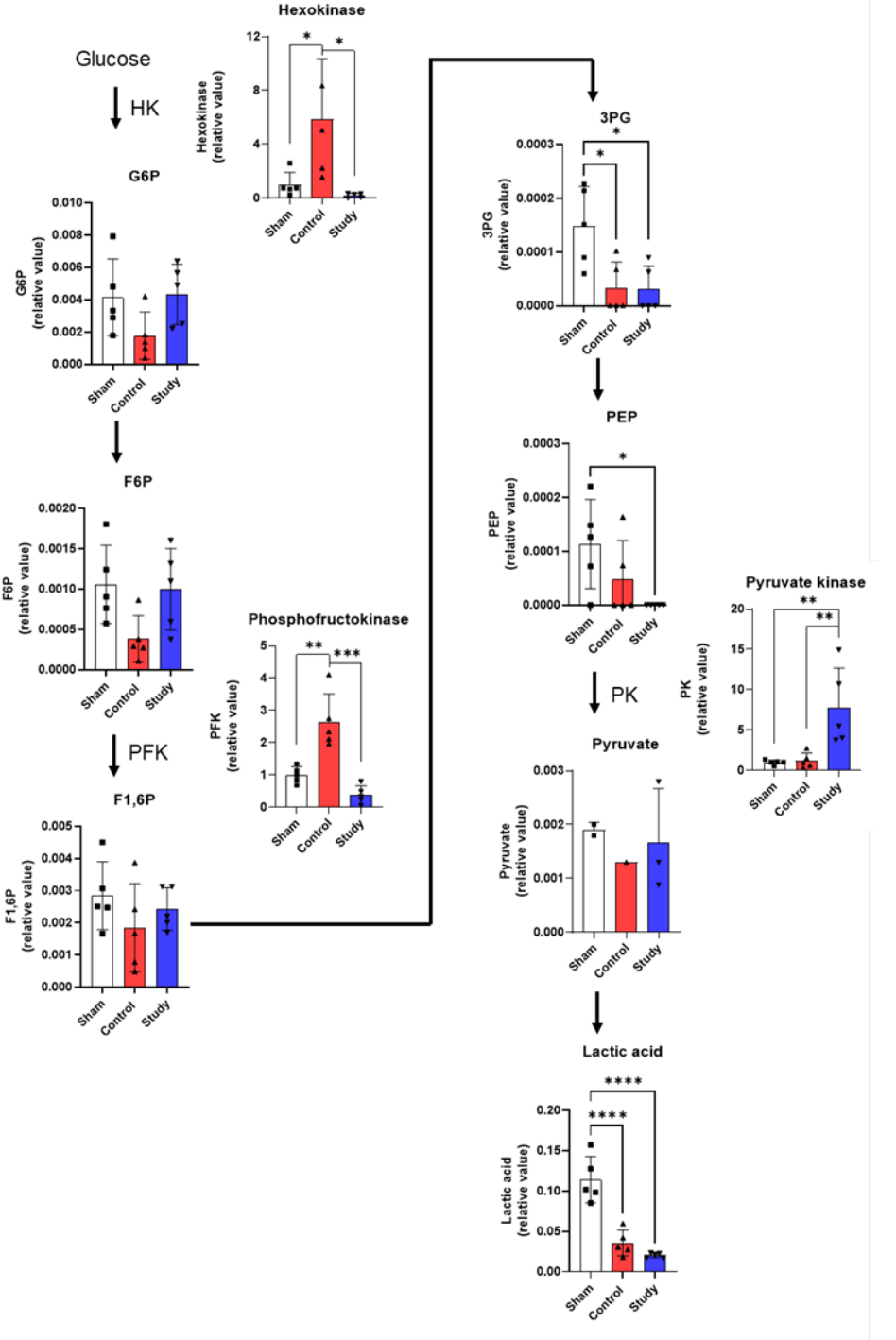

Figure 6. Metabolite levels in glycolysis pathways. Metabolites associated with glucose metabolism showed a lower tendency in control group than in study group (G6P, F6P, F1, 6P). HK and PFK, important enzymes in glycolysis, showed significantly increased expression in the control group than in the study group (* $p < 0.05$, ** $p < 0.01$, *** $p < 0.001$, and ****$p < 0.0001$).
HK, hexokinase; G6P, glucose-6- phosphate; F6P, fructose-6-phosphate; PFK, phosphofructokinase; F1,6P, fructose-1,6-bispohsphate; 3PG, 3-phosphoglycerate; PEP, phosphoenolpyruvate; PK, pyruvate kinase

B. TCA cycle

TCA cycle metabolites were not significantly different between the control and study groups (Figure 7), and showed similar trends in both. This result of the TCA cycle was thought to show similar energy conversion in both groups due to the inflow of acetyl CoA and succinyl CoA through branched-chain amino acid and beta-oxidation in addition to pyruvate.

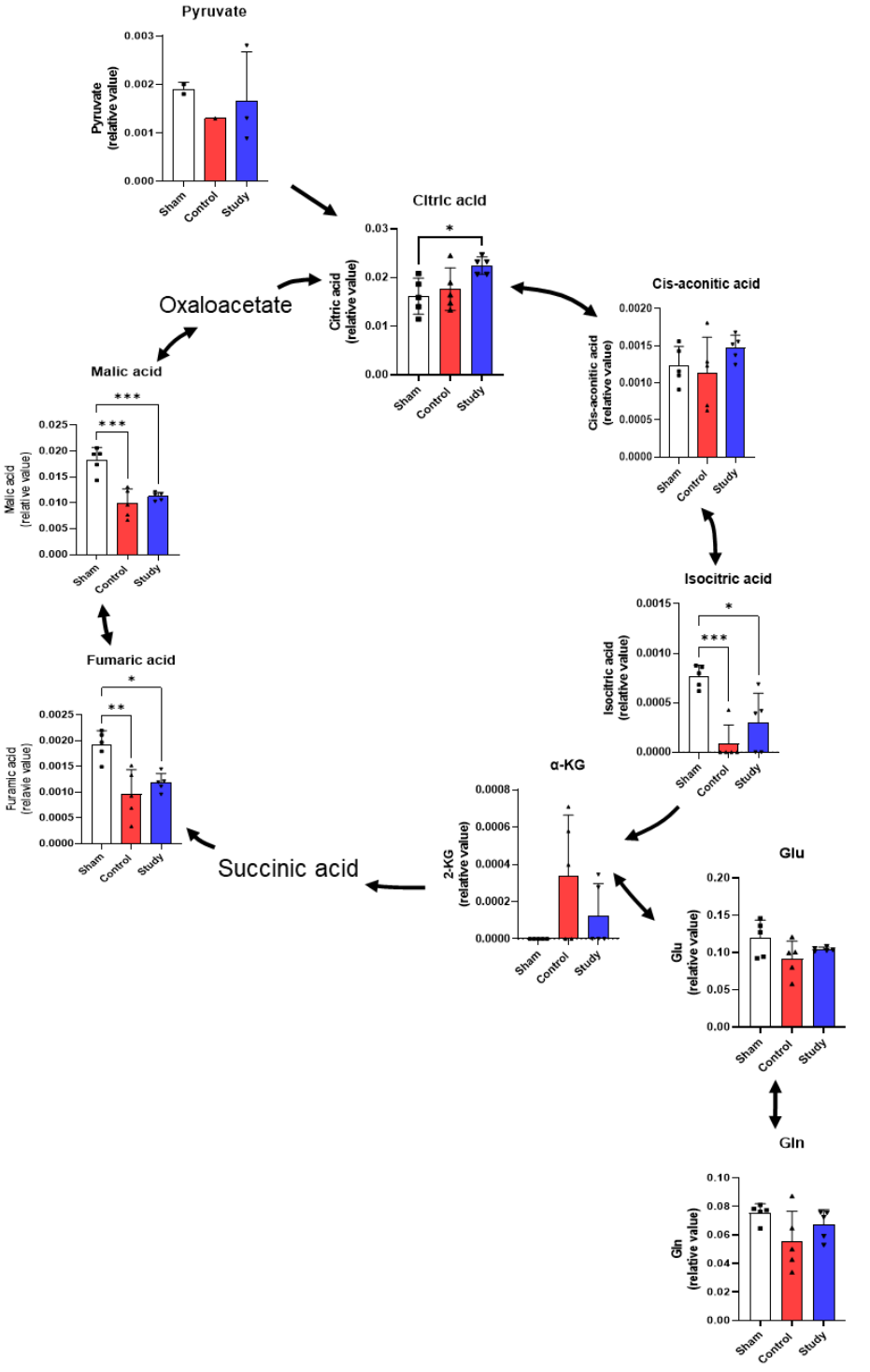

Figure 7. Metabolite levels in TCA cycle. The metabolites showed no significant difference.
αKG, α-ketoglutarate; Glu, glutamate; Gln, glutamic acid

5. mTORC- HIF1α- NLRP3 inflammasome pathway signaling

The expression level of mTORC (control vs. study, 4.092 vs. 0.2626; p =0.0011) and HIF-1α (control vs. study, 5.614 vs. 0.1616; p =0.0008) were significantly increased in the control group than in the study group. The expression level of NLRP3 inflammasome (control vs. study, 4.782 vs. 2.309; p =0.0572) tended to increase in the control group, though not significantly, than in the study group, but its main effector Caspase-1 (control vs. study, 2.798 vs. 0.3470; p =0.0004) was significantly increased in the control group than in the study group (Figure 8).

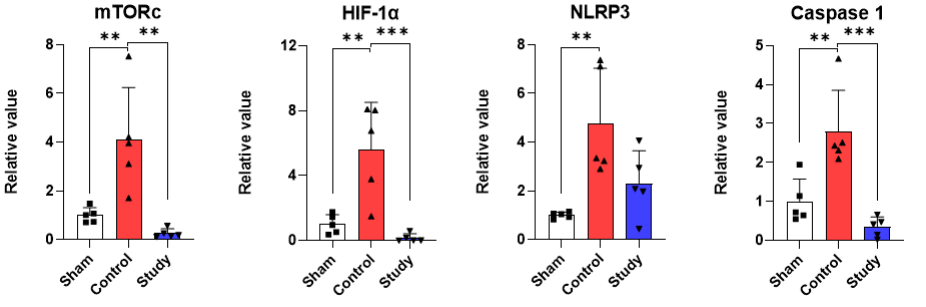

Figure 8. Expression level of mTORC, HIF-1α, NLRP3 and Caspase 1 in samples from sham, control, and study groups. HIF-1α expression was significantly increased in the control group than in the study group (** $p < 0.01$, *** $p < 0.001$).

The above results confirmed that mTORC was activated in normothermic EVLP, and thus HIF-1a expression and activity were increased under aerobic conditions, and this reaction was suppressed in subnormothermic EVLP. This leads to an increase in glycolysis in normothermic EVLPs compared to subnormothermic EVLP, which is consistent with previously identified results of glucose metabolism. In addition, it was shown that the expression of Caspase

1, a major effector, was increased in normothermic EVLP through activation of NLRP3 inflammasome, which is consistent with the previously confirmed increase in inflammatory cytokine secretion in normothermic EVLP group compared to subnormothermic EVLP.

IV. DISCUSSION

The concept of using EVLP to increase the rate of organ procurement is highly accepted due to the shortage of donor organs. The shortage is the primary limiting factor in the widespread use of lung transplants. Machine perfusion provides a continuous supply of oxygen and substrates. Previous studies had attempted to increase graft survival rates by increasing the number of available donor lungs through functional re-evaluations of marginal lungs and by improving graft functions through therapeutic modifications during EVLP. In some studies, normothermic EVLP was found to maintain stable donor graft function and show minimal EVLP-induced injuries [4,28]. Although a few studies have demonstrated the usefulness of subnormothermic EVLP recently [18,29,30], the perfusate temperature that would be favorable for lung preservation still remains unclear. Subnormothermic machine perfusion settings are already in clinical use for other solid organ, such as kidney [16,31] and liver [32], transplants. Studies have shown the former to be able to lower the rate of metabolism, reduce oxygen demand, and simultaneously enable the removal of metabolic waste product and restoration of ATP.

In this study, subnormothermic EVLP showed favorable results for OC and PVR compared to normothermic EVLP. The inflammatory cytokine levels supported the results. Inflammatory cytokines, such as TNF-α, IL-1ß, IL-6, and IL-18, were significantly higher in normothermic EVLP than in sham and subnormothermic EVLP. Additionally, caspase-3, an apoptotic marker, was significantly higher in normothermic EVLP than in sham and subnormothermic EVLP. Histologic evaluation showed subnormothermic EVLP to cause less lung injury than normothermic EVLP in terms of LIS. Briefly, subnormothermic EVLP has superior graft function, and less graft injury and inflammation than normothermic EVLP. Some recent studies on subnormothermic EVLP have also reported similar results. Arni et al. showed that an EVLP at 28 ℃ had more protective effect than normothermia, with a better physiological state of the DCD

donor graft after 4 h of ELVP [29]. Physiological data, including PVR, edema, compliance, and OC, were significantly improved at low perfusate temperatures, which was due to the improvement of tissue ATP content and decreased secretion of pro-inflammatory cytokines [29]. In another study conducted by the same authors, perfusion at normothermia was shown to have a strong potential benefit for both physiological parameters and attenuation of I/R injury in a rat model [30].

In this study, we considered the difference to be a protective effect of perfusate temperature, in addition to the effect of graft protection due to EVLP. Metabolomics is a postgenomic systems biology approach of diagnostic innovation that involves the measurement of a large number of metabolites using non-chemical and non-colorimetric methods [33]. In organ transplantation era, metabolomics is performed to monitor the severity of organ IRI and function during preservation [33]. The results can help in identifying innovative metabolite biomarkers for graft function or therapeutic intervention [33]. In a previous study, IR injury was found to occur when there was a change from aerobic to anaerobic metabolism due to brief post-ischemic reperfusion [34]. During ischemia, energy metabolism switched from fatty acid oxidation to oxidative glycolysis for ATP production [35,36]. During reperfusion, there was an increase in both lipid and protein oxidation over that before the ischemic insult [37]. Based on this evidence, we used metabolomics to identify the mechanism by which perfusate temperature affects graft protection.

‘Metabolic reprogramming’ is an altered configuration of cellular metabolism, in order to meet the specialized needs of cells exposed to stimuli or stressors [38]. Glycolysis and oxidative phosphorylation (OXPHOS) are some metabolic processes that generate ATP [39]. Anaerobic glycolysis is a less efficient process compared to OXPHOS, and is the preferred metabolic pathway in highly proliferative cells, such as in inflammation and cancer, although under aerobic conditions [39-42]. This metabolic change is called "Warburg effect", and refers to the fact that some cells rely on glycolysis for energy generation, even in aerobic

conditions[41]. During an inflammatory response, immune cells, such as macrophage and T cells, undergo this metabolic shift [41-43]; the inflammatory phase favors the anaerobic glycolysis process, and OXPHOS dominates in the resolution phase of inflammation [39].

Previous studies had shown that metabolic reprogramming in glycolysis promotes inflammatory response in an animal model of ALI. In mouse model of ALI, glycolysis is enhanced during ALI and augments the inflammatory response [44-46]. In murine model of ALI, PFK2 enzyme, involved in glycolysis, acts as an innate protective mechanism of alveolar epithelial cell metabolism [47], and glycolysis contributes to the profibrotic phenotype in lung [41]. The inflammatory phenotype, M1 macrophage, relies on glycolysis and breaks down in the TCA cycle in chronic lung disease [42]. In our study, HK and PFK, important enzymes involved in glycolysis, were significantly increased in the control group than in the study group, whereas glycolysis intermediate metabolites in the control group tended to decrease. Based on these results, we inferred that metabolic reprogramming occurs from the control group to the glycolytic process and the inflammatory response is intensified. The field of organ preservation has shown similar results. Aerobic glycolysis was decreased in subnormothermic EVLP [30] and lactate level was decreased in hypothermic machine perfusion in EVLP [30].

mTORC1 mainly maintains a cellular balance between anabolism and catabolism in response to environmental stimuli [48,49], and HIF-1α is an important transcription factor for cells to sense and adapt to changes in oxygen level [50]. HIF-1α-PFK2 axis appears to act as an innate protective mechanism for the critical intersection between alveolar epithelial cell metabolism and lung inflammation during ALI [47]. HIF1α and its target genes involved in glucose uptake and glycolysis are upregulated in mTORC1 signaling-dependent manner [40,49,51]; the glycolytic genes include GLUT1, HK, OFK, and PK [50,50]. mTORC1 activation alone increased HIF-1α levels at transcription and translation under normoxic conditions, without any effect on its stability [40,49]. Overexpression of HIF-1α

induces M1 marker upregulation and plays an important role in inflammatory macrophage function [50]. Activated macrophages result in a metabolic shift to aerobic glycolysis, with HIF-1α accumulation playing an essential role in this shift [50]. Glycolysis via mTORC1 activation is an important pathway related to NLRP3 inflammasome activation in macrophages [44,45]. At the end of this pathway, secretion of inflammatory cytokines, such as IL-1ß, IL-18, and IL-6, was increased, indicating a proinflammatory condition [45,50]. Overall, it was confirmed in ALI (a chronic lung disease), that metabolic reprogramming to glycolysis exerts an inflammatory effect through the mTORC1-HIF-1α-NLRP3 inflammasome axis, as reported in previous studies. In our study, the expression level of HIF-1α was increased in the control group than in the study group. Expression of NLRP3 also tended to increase in the control group than in the study group; however, it was not significant, possibly due to small sample numbers. Therefore, we inferred that this pathway is related to increased inflammatory response through increase in glycolysis.

Considering the changes in metabolomics, proinflammatory cytokines, and graft function mentioned above, the protective effect of subnormothermic EVLP was thought to be due to the metabolic shift to glycolysis. Compared to the subnormothermic EVLP group, normothermic EVLP group uses glycolysis more predominantly as the way of energy metabolism. In normothermic EVLP, the change in glycolytic phenotype occurs through the mTORC1-HIF-1α-NLRP3 pathway, especially via HIF-1α, and the secretion of inflammatory cytokines through this causes deterioration of graft function. The changes were attenuated through subnormothermia, showing a graft protective effect.

In our study, subnormothermic EVLP showed a sham-like pattern and normothermic EVLP caused more lung injury. These results are because IRI causes injury during reperfusion more than ischemia itself. In previous studies, it was already known that IRI was initiated by the rapid and robust generation of reactive oxygen species in the reperfusion phase rather than the ischemia phase

[52]. In other words, lung injury due to reperfusion occurs during EVLP, and this reperfusion injury is might to be affected by the temperature of the perfusate, and the subnormothermic condition is thought to cause less injury due to this reperfusion than the normothermic condition.

This study, however, has some limitations. First, since this study was regarding the function and metabolites of rat lung grafts after EVLP, it did not assess the graft function after in-vivo reperfusion. Secondly, although subnormothermic conditions showed improvements in graft function during EVLP, it was difficult to clarify the mechanism related to it. Significant changes were seen in glycolysis pathway, but statistical power was not strong owing to the small sample size.

V. CONCLUSION

Our study provided a schematic overview of the glycolytic pathways in lung ischemia reperfusion and identified the effect of perfusate temperature on IRI during EVLP. Subnormothermic EVLP was confirmed to show better graft function than normothermic EVLP. This may have been due to the metabolic change, since subnormothermic EVLP especially showed superior graft function by decreased expression of a proinflammatory cytokine through inhibition of glycolysis via mTOC1-HIF-1α-NLRP3 inflammasome pathway. Studies to confirm the metabolic pathway required for a therapeutic target should be conducted in future by identifying the appropriate perfusate temperature in the EVLP protocol.

REFERENCES

1. George TJ, Arnaiutakis GJ, Beaty CA, Jandu SK, Santhanam L, Berkowitz DE, et al. A physiologic and biochemical profile of clinically rejected lungs on a normothermic *ex vivo* lung perfusion platform. J Surg Res, 2013; 183.1: 75-83.
2. Sadaria MR, Smith PD, Fullerton DA, Justison GA, Lee JH, Puskas F, et al. Cytokine expression profile in human lungs undergoing normothermic *ex-vivo* lung perfusion. Ann Thorac Surg, 2011; 92.2: 478-84.
3. Pan X, Yang J, Fu S, Zhao H. Application of *ex vivo* lung perfusion (EVLP) in lung transplantation. J Thorac Dis, 2018; 10.7: 4637-42.
4. Cypel M, Yeung JC, Liu M, Anraku M, Chen F, Karolak W, et al. Normothermic *ex vivo* lung perfusion in clinical lung transplantation. N Engl J Med, 2011; 364.15: 1431-40.
5. Cypel M. *Ex vivo* lung perfusion (EVLP). Curr Respir Care Rep, 2013; 2.3: 167-72.
6. Burki S, Noda K, Kumar A, Philips B, Sanchez PG, D'Cunha J. Influence of various perfusion temperatures on lung graft preservation during *ex vivo* lung perfusion. J Heart Lung Transplant, 2019; 38.4: S240-1.
7. Citak N, Arni S, Cehn J, Ceulemans L, Schmitt-Opitz I, Inci I. Subnormothermic *ex vivo* lung perfusion improves graft preservation in rat *ex vivo* lung perfusion model. J Heart Lung Transplant, 2020; 39.4: S354.
8. Maeyashiki T, Arni S, Iskender I, Weder W, Inci I. Sub-normothermic *ex-vivo* lung perfusion attenuates ischemia reperfusion injury from donation after circulatory death donors. J Heart Lung Transplant, 2019; 38.4: S237.
9. Yeung JC, Zamel R, Klement W, Bai XH, Machuca TN, Waddell TK, et al. Towards donor lung recovery-gene expression changes during *ex vivo* lung perfusion of human lungs. Am J Transplant, 2018; 18.6: 1518-26.

10. Hsin M, Au T. *Ex vivo* lung perfusion: a potential platform for molecular diagnosis and *ex vivo* organ repair. J Thorac Dis, 2018; 10.S16: S1871-83.
11. Dromparis P, Aboelnazar NS, Wagner S, Himmat S, White CW, Hatami S, et al. *Ex vivo* perfusion induces a time- and perfusate-dependent molecular repair response in explanted porcine lungs. Am J Transplant, 2019; 19.4: 1024-36.
12. Wallinder A, Ricksten SE, Silverborn M, Hansson C, Riise GC, Liden H, et al. Early results in transplantation of initially rejected donor lungs after *ex vivo* lung perfusion: a case-control study. Eur J Cardiothorac Surg, 2014; 45.1: 40-5.
13. Sage E, Mussot S, Trebbia G, Puyo P, Stern M, Dartevelle P, et al. Lung transplantation from initially rejected donors after *ex vivo* lung reconditioning: the French experience. Eur J Cardiothorac Surg, 2014; 46.5: 794-9.
14. Bozso S, Freed D, Nagendran J. Successful transplantation of extended criteria lungs after prolongedex vivolung perfusion performed on a portable device. Transpl Int, 2015; 28.2: 248-50.
15. Zeriouh M, Sabashnikov A, Mohite PN, Zych B, Patil NP, García-Sáez D, et al. Utilization of the organ care system for bilateral lung transplantation: preliminary results of a comparative study. Interact Cardiovasc Thorac Surg, 2016; 23.3: 351-7.
16. Patel K, Smith TB, Neil DA, Thakker A, Tsuchiya Y, Higgs EB, Ludwig C. The effects of oxygenation on *ex vivo* kidneys undergoing hypothermic machine perfusion. Transplantation, 2019; 103.2: 314-22.
17. Rojas-Pena A, Robert HB. *Ex situ* organ preservation: the temperature paradigm. Transplantation, 2018; 102.4: 554-6.
18. Gloria JN, Yerxa J, Kesseli SJ, Davis RP, Samoylova ML, Barbas AS, et al. Subnormothermic *ex vivo* lung perfusion attenuates graft

inflammation in a rat transplant model. J Thorac Cardiovasc Surg, 2021; S0022-5223(21)00165-3.

19. Liu Y, Yan S, Ji C, Dai W, Hu W, Zhang W, et al. Metabolomic changes and protective effect of (L)-carnitine in rat kidney ischemia/reperfusion injury. Kidney Blood Press Res, 2012; 35.5: 373-81.
20. Wishart DS. Metabolomics: the principles and potential applications to transplantation. Am J Transplant, 2005; 5.12: 2814-20.
21. Wyss RK, Méndez Carmona N, Arnold M, Segiser A, Mueller M, Dutkowski P, et al. Hypothermic, oxygenated perfusion (HOPE) provides cardioprotection *via* succinate oxidation prior to normothermic perfusion in a rat model of donation after circulatory death (DCD). Am J Transplant, 2021; 21.3: 1003-11.
22. Schlegel A, Muller X, Dutkowski P. Hypothermic machine preservation of the liver: state of the art. Curr Transplant Rep, 2018; 5.1: 93-102.
23. Noda K, Shigemura N, Tanaka Y, Bhama JK, D'Cunha,J, Luketich JD, et al. Successful prolonged *ex vivo* lung perfusion for graft preservation in rats. Eur J Cardiothorac Surg, 2014; 45.3: e54-60.
24. Haam S, Noda K, Philips BJ, Harano T, Sanchez PG, Shigemura N. Cyclosporin A administration during *ex vivo* lung perfusion preserves lung grafts in rat transplant model. Transplantation, 2020; 104.9: e252-9.
25. Nishina K, Mikawa K, Takao Y, Maekawa N, Shiga M, Obara H. ONO-5046, an elastase inhibitor, attenuates endotoxin-induced acute lung injury in rabbits. Anesth Analg, 1997; 84.5: 1097-103.
26. Haam S, Lee JG, Paik HC, Park MS, Lim BJ. Hydrogen gas inhalation during *ex vivo* lung perfusion of donor lungs recovered after cardiac death. J Heart Lung Transplant, 2018; 37.10: 1271-8.
27. Yamamoto H, Fujimori T, Sato H, Ishikawa G, Kami K, Ohashi Y. Statistical hypothesis testing of factor loading in principal component analysis and its application to metabolite set enrichment analysis. BMC

Bioinformatics, 2014; 15.1: 1-9.

28. Cypel M, Yeung JC, Hirayama S, Rubacha M, Fischer S, Anraku M, et al. Technique for prolonged normothermic *ex vivo* lung perfusion. J Heart Lung Transplant, 2008; 27.12: 1319-25.
29. Arni S, Maeyashiki T, Opitz I, Inci I. Subnormothermic *ex vivo* lung perfusion attenuates ischemia reperfusion injury from donation after circulatory death donors. PLoS One, 2021; 16.8: e0255155.
30. Arni S, Maeyashiki T, Citak N, Opitz I, Inci I. Subnormothermic *ex vivo* lung perfusion temperature improves graft preservation in lung transplantation. Cells, 2021; 10.4: 748.
31. Kataria A, Magoon S, Makkar B, Gundroo A. Machine perfusion in kidney transplantation. Curr Opin Organ Transplant, 2019; 24.4: 378-84.
32. Schlegel A, Dutkowski P. Role of hypothermic machine perfusion in liver transplantation. Transpl Int, 2015; 28.6: 677-89.
33. Kvietkauskas M, Zitkute V, Leber B, Strupas K, Stiegler P, Schemmer P. The role of metabolomics in current concepts of organ preservation. Int J Mol Sci, 2020; 21.18: 6607.
34. Erpicum P, Rowart P, Defraigne JO, Krzesinski JM, Jouret F. What we need to know about lipid-associated injury in case of renal ischemia-reperfusion. Am J Renal Physiol, 2018; 315.6: F1714-9.
35. Buchko MT, Stewart CJ, Hatami S, Himmat S, Freed DH, Nagendran J. Total parenteral nutrition in *ex vivo* lung perfusion: addressing metabolism improves both inflammation and oxygenation. Am J Transplant, 2019; 19.12: 3390-7.
36. Eltzschig HK, Eckle T. Ischemia and reperfusion – from mechanism to translation. Nat Med, 2011; 17.11: 1391-401.
37. Ayene IS, Dodia C, Fisher AB. Role of oxygen in oxidation of lipid and protein during ischemia/reperfusion in isolated perfused rat lung. Arch Biochem Biophys, 1992; 296.1: 183-9.

38. Aboushousha R, Elko E, Chia SB, Manuel AM, Wetering CV, Velden JV, et al. Glutathionylation chemistry promotes interleukin-1 beta-mediated glycolytic reprogramming and pro-inflammatory signaling in lung epithelial cells. FASEB J, 2021; 35.5: e21525.

39. Soto-Heredero G, Gomez de las Heras MM, Gabandé-Rodríguez E, Oller J, Mittelbrunn M. Glycolysis - a key player in the inflammatory response. FEBS J, 2020; 287.16: 3350-69.

40. Magaway C, Kim E, Jacinto E. Targeting mTOR and metabolism in cancer: lessons and innovations. Cells, 2019; 8: 1584.

41. Zhao H, Dennery PA, Yao H. Metabolic reprogramming in the pathogenesis of chronic lung diseases, including BPD, COPD, and pulmonary fibrosis. Am J Physiol Lung Cell Mol Physiol, 2018; 314.4: L544-54.

42. Ogger PP, Byrne AJ. Macrophage metabolic reprogramming during chronic lung disease. Mucosal Immunol, 2021; 14.2: 282-95.

43. Bossche J, O'Neill LA, Menon D. Macrophage immunometabolism: where are we (going)? Trends Immunol, 2017; 38.6: 395-406.

44. Zhong WJ, Yang HH, Guan XX, Xiong JB, Sun CC, Zhang CY, et al. Inhibition of glycolysis alleviates lipopolysaccharide-induced acute lung injury in a mouse model. J Cell Physiol, 2019; 234.4: 4641-54.

45. Moon JS, Hisata S, Park MA, DeNicola GM, Ryter SW, Nakahira K, et al. mTORC1-induced HK1-dependent glycolysis regulates NLRP3 inflammasome activation. Cell Rep, 2015; 12.1: 102-15.

46. Gong Y, Lan H, Yu Z, Wang M, Wang S, Chen Y, et al. Blockage of glycolysis by targeting PFKFB3 alleviates sepsis-related acute lung injury via suppressing inflammation and apoptosis of alveolar epithelial cells. Biochem Biophys Res Commun, 2017; 491.2: 522-9.

47. Vohwinkel C, Burns N, Kraynik J, Stenmark KR, Eltzschig H. Critical role of phosphofructokinase-2 fructose-2,6-bisphosphatase (pfkfb) 3 in acute lung injury. Am J Respir Crit Care Med, 2016; A7492.

48. Mao Z, Zhang W. Role of mTOR in glucose and lipid metabolism. Int J Mol Sci, 2018; 19.7: 2043.

49. Yecies JL, Manning BD. Transcriptional control of cellular metabolism by mTOR signaling. Cancer Res, 2011; 71.8: 2815-20.

50. McGettrick AF, O'Neill LA. The role of HIF in immunity and inflammation. Cell Metab, 2020; 32.4: 524-36.

51. Duvel K, Yecies JL, Menon S, Raman P, Lipovsky AI, Souza AL, et al. Activation of a metabolic gene regulatory network downstream of mTOR complex 1. Mol Cell, 2010; 39.2: 171-83.

52. Laubach VE, Sharma AK. Mechanisms of lung ischemia-reperfusion injury. Current opinion in organ transplantation, 2016; 21.3: 246-52.

APPENDICES

EVLP, *ex-vivo* lung perfusion; PA, pulmonary artery; FiO_2, fraction of inspired oxygen; OC, oxygen capacity; LA, left atrium PO_2, partial pressure of oxygen; PA, pulmonary artery; PVR, pulmonary vascular resistance; PAP, peak airway pressure; CE-TOFMS, capillary electrophoresis- time-of-flight mass spectrometry; ESI-MS, electrospray ionization-mass spectrometry; MT, migration time; HMT, human metabolome technology; HCA, hierarchical cluster analysis; PCA, principal component analysis; qRT-PCR, quantitative reverse transcription-polymerase chain reaction; IL, interleukin; TNF-α, tumor necrosis factor-alpha

Abstract (In Korean)

체외폐 관류 (*Ex vivo* lung perfusion) 시 관류액의 온도변화에 따른 폐 이식편의 생리적 및 대사적 변화

<지도교수 백효채>

연세대학교 대학원 의학과

서지원

목적: 체외폐 관류 (EVLP)는 이식을 위해 기증자 폐를 평가하고 손상에서 복구하는데 유용한 기술로, 허혈-재관류 손상으로부터 폐구득률을 높이고 이식편 기능 장애를 줄일 수 있다. 그러나 이식폐의 기능에 대한 관류 온도의 영향을 보여주는 연구는 제한적이다. 이 연구에서 우리는 생체 외 폐 관류 동안 정상체온이하의 관류액 온도가 대사체학 측면에서 기증자 폐 기능과 허혈-재관류 손상에 어떻게 영향을 미치는지 조사하였다.
방법: 15마리의 수컷 Sprague-Dawley 쥐를 무작위로 세 그룹으로 나누었다: 무처리 (무처리군, n = 5), 정상 체온 하 체외폐 관류 (37°C, 대조군, n = 5), 정상체온이하 체외폐 관류 (30°C, 연구군, n = 5). OC, compliance, PVR 을 통하여 폐 기능 분석을

수행하였으며, 염증성 사이토카인의 발현 수준 및 해당과정의 효소와 mTORC1 pathway 관련 유전자 발현을 평가하였다. capillary electrophoresis Time-of-Flight Mass Spectrometry를 사용하여 각 그룹의 폐 조직에서 대사체 분석을 수행하였다.

결과: OC 및 PVR을 포함한 기능적 매개변수는 체외폐 관류 동안 연구군이 대조군보다 통계적으로 유의하게 우수했습니다. IL-6,18,1ß 및 TNF-α와 같은 염증성 사이토카인의 발현 수준은 연구군보다 대조군에서 유의하게 증가하였다. 대사체 분석은 해당 연구 그룹에서 연구 그룹보다 해당 작용이 유의하게 감소한 것으로 나타났습니다. mTORC-HIF-1α-NLRP3 pathway 관련 유전자는 연구군보다 대조군에서 발현이 유의하게 증가하였다.

결 론: 본 연구에서는 정상체온이하의 체외폐 관류가 정상온도의 체외폐 관류에 비해 이식편 기능이 더 우수함을 확인하였다. 정상체온이하의 체외폐 관류는 정상온도 의 체외폐 관류보다 mTORC1-HIF1α-glycolysis 경로의 억제로 인한 해당과정의 억제를 통해 전염증성 사이토카인의 발현을 감소시켜 우수한 이식 기능을 보여주었다.

핵심되는 말: *ex-vivo* lung perfusion, temperature, lung transplantation, metabolomics, glycolysis